第 35 卷第 7 期
2019 年 7 月

无 机 化 学 学 报
CHINESE JOURNAL OF INORGANIC CHEMISTRY

Vol.35 No.7
1267-1274

# 基于水相稳定和甲基修饰的二维锌框架化合物：合成，表征及药物缓释功能

闫晓霖[1] 郭海福*[,2] 闫 鹏[2] 朱佳敏[2] 王 莹[2] 谭嘉美[2] 丁 敏[2] 郑泳锐[2]

([1]内蒙古农业大学理学院，呼和浩特 010018)

([2]肇庆学院环境与化学工程学院，肇庆 526061)

**摘要**：采用甲基修饰的含氮辅助配体，与间苯二甲酸和六水硝酸锌在水热条件下合成一个水相稳定的金属有机框架物：{[Zn(BDC)(dmbpy)]·$4H_2O$}$_n$ (**1**)(BDC=间苯二甲酸，dmbpy=3，3′-二甲基-4，4′-联吡啶)，并对该化合物进行结构表征。X 射线粉末衍射和差热分析结果显示该化合物表现出良好的热稳定性和水相稳定性。化合物 **1** 为二维结构，沿 *b* 轴方向存在 0.92 nm×0.83 nm 和 0.82 nm×0.39 nm 的孔道。该化合物对 5-氟尿嘧啶的包封率(质量分数)高达 14.2%，并且在模拟体液中可缓慢释放 70 h (37 ℃下，释放率在 pH 值为 7.4 和 6.0 时分别为 94.5%和 99%)。体内斑马鱼和体外 MTT 法结果显示该化合物浓度达到 500 μg·$mL^{-1}$ 时生理依然安全。

**关键词**：锌框架化合物；水相稳定；合成；表征；药物缓释

**中图分类号**：O614.24+1 **文献标识码**：A **文章编号**：1001-4861(2019)07-1267-08

**DOI**：10.11862/CJIC.2019.137

# Synthesis, Characterization and Drug Delivery of a Water-Stable and Methyl-Functionalized 2D Zinc(Ⅱ) Metal-Organic Framework

YAN Xiao-Lin[1] GUO Hai-Fu*[,2] YAN Peng[2] ZHU Jia-Min[2] WANG Ying[2]

TAN Jia-Mei[2] DING Min[2] ZHENG Yong-Rui[2]

([1]*College of Science, Inner Mongolia Agricultural University, Huhhot* 010018, *China*)

([2]*School of Environmental and Chemical Engineering, Zhaoqing University, Zhaoqing, Guangdong* 526061, *China*)

**Abstract:** By using a methyl-functionalized N-donor ligand, a water-stable zinc-based MOF {[Zn(BDC)(dmbpy)]·$4H_2O$}$_n$ (**1**) (BDC=isophthalate, dmbpy=3,3′-dimethyl-4,4′-bipyridine) was synthesized and structurally characterized. TGA and PXRD results show high thermal and water stability for **1**. **1** exhibits a 2D (4,4) net with channels of 0.92 nm×0.83 nm and 0.82 nm×0.39 nm along the *b* axis, respectively. De-solvated **1** adsorbs around 14.2%(*w*/*w*) 5-fluorouracil (5-FU) and the cumulative release value of 5-FU after 70 h was about 94.5% and 99% in PBS (pH=7.4 and pH=6.0) at 37 ℃, respectively. The *in vivo* zebrafish toxicity tests and *in vitro* MTT assays of **1** at different concentrations results reveal that **1** is nontoxic (cell viability>80%) up to concentrations of 500 μg·$mL^{-1}$. CCDC: 1823293.

**Keywords:** zinc-organic framework; water-stable; synthesis; characterization; drug delivery

收稿日期：2018-12-18。收修改稿日期：2019-04-03。

内蒙古自治区自然科学基金(No.2015MS0209)和大学生创新创业训练计划项目(No.201710580057)资助。

*通信联系人。E-mail：guohaifu@sina.com

## 0 Introduction

Metal-organic frameworks have received widespread attention over the past decade owing to their modular assembly, structural diversity and fascinating topology, chemical tailorability and tenability, as well as their potential in gas storage and separation [1-2], nonlinear optics [3], catalysis [4], magnetism [5], luminescence [6], drug delivery [7], sensing [8], and detection [9-10], etc. However, reports have shown that some of zinc-based MOFs are unstable and lose their structural integrity and high surface areas rapidly when were exposed to air[11]. This drawback greatly hinders the practical applications of the MOFs because moisture is ubiquitous in the environment. Meanwhile, MOFs as drug-delivery carriers are highly desirable due to their large loadings and controlled release of drugs [12]. Compared to the other drug carriers, the MOFs/drug systems possessed a stronger interaction, which consist of hydrogen bonds, coordination bonds, and anions-cations electrostatic interaction between drugs and frameworks, to achieve stable drug release profiles and drug concentration[13]. However, for biomedical applications, the biocompatibility and the stability in water solution of MOFs are important. Some MOFs may present concerns owing to potential leaching of toxic metal ions ($Cr^{3+}$, $Cd^{2+}$, *etc.*) and other harmful constituents[14].

With this in mind, we prepared a new 2D Zn-MOF constructed from isophthalate and 3,3′-dimethyl-4,4′-bipyridine decorated by methyl groups, which adsorbs around 14.2%(*w*/*w*) 5-fluorouracil (5-FU). The *in vivo* zebrafish toxicity tests and *in vitro* MTT assays of **1** reveal that **1** is nontoxic.

## 1 Experimental

### 1.1 Materials and measurements

Reagent grade 5-FU (99%), isophthalic acid ($H_2BDC$) and $Zn(NO_3)_2\cdot 6H_2O$ metal salt were obtained from Aladdin and used as received. 3,3′-dimethyl-4,4′-bipyridine (dmbpy) was synthesized according to the reported procedures[11]. Dialysis bag (Molecular weight cut-off: 500) were obtained from Aladdin and used as received. Acetonitrile, trifluoroacetic acid, methanol used were HPLC grade and obtained from Sigma-Aldrich (St. Louis, USA). The water used for HPLC was double distilled water. Elemental analyses for C, H, and N were carried out using a Vario EL Ⅲ Elemental Analyzer. Infrared spectra were recorded (4 000~400 $cm^{-1}$) as KBr disks on a Bruker 1600 FTIR spectrometer. Thermogravimetric analyses (TGA) were carried out on an automatic simultaneous thermal analyzer (DTG-60, Shimadzu) under $N_2$ atmosphere at a heating rate of 10 ℃·$min^{-1}$ within a temperature range of 25~800 ℃. Powder XRD investigations were carried out on a Bruker AXS D8-Advanced diffractometer at 40 kV and 40 mA with Cu $K\alpha$ ($\lambda$=0.154 06 nm) radiation ($2\theta$=5°~40°). The $N_2$ isotherm was measured with an automatic volumetric adsorption apparatus (Micrometrics ASAP 2020) at 77 K.

HPLC analyses were carried out on an Agilent 1260 liquid chromatography system equipped with a UV-Vis detector and the detection wavelength was 265 nm. Ultimate XB-C18 (4.6 mm×250 mm, 5 μm, Welch materials) was used as analytical column for separation. The mobile phase was comprised of acetonitrile and 0.1% trifluoroacetic-water (pH 2.5, 97:3, *V*/*V*) at a flow rate of 1.0 mL·$min^{-1}$. The column temperature was set at 30℃.

### 1.2 Synthesis of 1

A mixture of $Zn(NO_3)_2\cdot 6H_2O$ (0.089 g, 0.3 mmol), isophthalic acid (0.050 3 g, 0.3 mmol), 3,3′-dimethyl-4,4′-bipyridine (0.028 g, 0.15 mmol), and $H_2O$ (10 mL) were sealed in a 23 mL Teflon reactor and kept under autogenous pressure at 150 ℃ for 3 days. Colorless single crystals were obtained (Yield: 55%, based on BDC) upon cooling the solution to room temperature at a rate of 5 ℃·$h^{-1}$. Anal. Calcd. for $C_{20}H_{24}N_2O_8Zn$(%): C, 49.4; H, 4.9; N, 5.8. Found(%): C, 50.1; H, 4.6; N, 6.2. IR (KBr, $cm^{-1}$): 3 387 (vs), 3 012 (m), 2 958(w), 1 610(vs), 1 562(s), 1 478(m), 1 453(w), 1 357(vs), 1 193(m), 1 148(w), 1 084(s), 936(w), 855(m), 831(m), 751(vs), 719(s), 659(m), 595(m), 450(w), 421(w) (Fig.S1).

### 1.3 Crystal structure analysis

Single crystal data for compound **1** was collected

on a Bruker Apex Ⅱ CCD diffractometer equipped at 50 kV and 30 mA with Mo $K\alpha$ radiation ($\lambda$=0.071 073 nm). Data collection and reduction were performed using the APEX Ⅱ software[15]. The structure was solved using direct methods followed by least-squares on $F^2$ using SHELXTL[16]. Non-hydrogen atoms were refined with independent anisotropic displacement parameters and hydrogen atoms attached to carbon were placed geometrically and refined using the riding model. The routine SQUEEZE (PLATON)[17] was applied to remove diffuse electron density caused by badly disordered water molecules. The formula unit was obtained based on the elemental analyses, IR spectra and thermogravimetric characterization. Crystal data, as well as details of data collection and refinement for **1** is summarized in Table 1. Selected bond lengths and angles, and H-bonding parameters for the compound are given in Table 2 and 3, respectively.

CCDC: 1823293.

**Table 1　Crystal data and structure refinement information for compound 1**

| | | | |
|---|---|---|---|
| Empirical formula | $C_{20}H_{16}N_2O_4Zn$ | *D*c / (Mg·m$^{-3}$) | 1.248 |
| Formula weight | 413.72 | Limiting indices | $-24 \leqslant h \leqslant 24, -14 \leqslant k \leqslant 7, -20 \leqslant l \leqslant 20$ |
| Temperature /K | 296(2) | Reflection collected, unique | 11 193, 1 420 |
| Size / mm | 0.29×0.24×0.17 | $R_{int}$ | 0.138 5 |
| Crystal system | Orthorhombic | *F*(000) | 1 696 |
| Space group | *Cmca* | $\theta$ range / (°) | 2.01~25.11 |
| *a* / nm | 2.027 3(8) | Goodness-of-fit on $F^2$ | 1.040 |
| *b* / nm | 1.260 0(6) | $R^*$ [$I>2\sigma(I)$] | $R_1$=0.053 0, $wR_2$=0.127 4 |
| *c* / nm | 1.723 5(11) | *R* (all data) | $R_1$=0.076 0, $wR_2$=0.137 6 |
| *V* / nm$^3$ | 4.403(4) | Largest diff. peak and hole / (e·nm$^{-3}$) | 690, −1 020 |
| *Z* | 8 | | |

* $R=\sum(||F_o|-|F_c||)/\sum|F_o|$; $wR=[\sum w(F_o^2-F_c^2)^2/\sum w(F_o)^2]^{1/2}$.

**Table 2　Selected bond lengths (nm) and angles (°) of 1**

| | | | | | |
|---|---|---|---|---|---|
| Zn(1)-O(2) | 0.198 2(3) | Zn(1)-N(1) | 0.204 9(3) | | |
| O(2)-Zn(1)-O(2)$^i$ | 100.55(17) | O(2)-Zn(1)-N(1) | 111.04(11) | O(2)$^i$-Zn(1)-N(1) | 116.31(11) |
| N(1)$^i$-Zn(1)-N(1) | 102.26(18) | | | | |

Symmetry codes: $^i$ 0.5−*x*, *y*, 0.5−*z*.

**Table 3　Hydrogen bond geometries for 1**

| D−H···A | *d*(D-H) / nm | *d*(H···A) / nm | *d*(D···A) / nm | ∠DHA / (°) |
|---|---|---|---|---|
| C13−H13···O1 | 0.093 | 0.256 | 0.303 9(3) | 112 |
| C13−H13···O2$^{ii}$ | 0.093 | 0.274 | 0.338 0(6) | 125 |

Symmetry codes: $^{ii}$ 0.5−*x*, 0.5+*y*, *z*.

### 1.4　Encapsulation of 5-FU and determination of encapsulation efficiency

The freeze-drying method was used to prepare 5-FU-loaded desolvated **1** (**1a**) materials. Briefly, 5-FU solution was prepared by dissolving 5 mg of 5-FU into 10 mL of methanol, then 10 mg of **1a** ($m_{5\text{-FU}}$:$m_{\mathbf{1a}}$=1:2) was added into solution and vortexed at 3 000 r·min$^{-1}$ for 20 min to obtain the suspension solution. Subsequently, the mixtures was vacuum freeze-dried for 12 h to achieve the 5-FU-loaded 1a materials. The experiment was carried out three times. The amount of 5-FU adsorbed into the porous solids of **1a** was estimated by HPLC. **1a** before and after the 5-FU entrapping were characterized by FT-IR and powder X-ray diffraction.

The HPLC method was used to evaluate the

entrapment efficiency (EE) of 5-FU in **1a**. Briefly, 2 mL of methanol was added to the inclusion compound and vortexed at 2 000 r·min$^{-1}$ for 5 min. Then the mixture was centrifuged at 12 000 r·min$^{-1}$ for 15 min. Subsequently, the supernatant was collected and the 5-FU concentration in the samples was determined by the HPLC method as mentioned above. The calibration curve of absorption (Abs) versus 5-FU concentration ($C$) was plotted as Abs=32.293$C$−184.9 ($R^2$=0.999 1)[18].

The encapsulation efficiency (EE) and loading capacity (LC) of 5-FU were calculated from the following formula:

$$EE=\frac{m_{t,\ 5\text{-}FU}-m_{f,\ 5\text{-}FU}}{m_{t,\ 5\text{-}FU}}\times 100\%$$

$$LC=\frac{m_{t,\ 5\text{-}FU}-m_{f,\ 5\text{-}FU}}{m_{\mathbf{1a}}}\times 100\%$$

Where $m_{t,5\text{-}FU}$ is the total mass of 5-Fu; $m_{f,5\text{-}FU}$ is the mass of free 5-FU; $m_{\mathbf{1a}}$ is the mass of **1a**.

### 1.5 5-FU release

The *in vitro* release of 5-FU from 1a was investigated by the dialysis method. The 5-FU -loaded **1a** samples (2 mL) were placed in a dialysis bag and then incubated in 60 mL of release medium (PBS, pH=7.4 or pH=6.0) with shaking at 60 r·min$^{-1}$ and 37 ℃ for at least three days. Then 1 mL of the release medium was collected at designated intervals at 0, 1, 2, 4, 6, 8, 10, 12, 24, 36, 48 and 72 h to test the concentration of 5-FU by HPLC at a wavelength of 265 nm. Meanwhile equal volume of fresh medium was added into the system. The released amount of 5-FU was calculated as the following formula:

$$M_i=C_iV+\sum_{n=1}^{i}C_nV_1$$

Where $M_i$ represents the accumulated release amount of 5-FU at each time points; $C_i$ and $C_n$ represent the concentration of 5-FU at each time point; $V_1$ represents the volume of collected release medium at each time point. All experiments were performed in triplicate.

### 1.6 *In vitro* cytotoxicity studies

The toxicity of **1** towards NIH-3T3, HEK-293, A549 and HEPG2 cells was determined using MTT assays in 96-well flat-bottom microtiter plates with seven different concentrations (0, 0.005, 0.05, 0.5, 5, 50 and 500 μg·mL$^{-1}$). After incubation for 24 and 48 h, the chemosensitivity was determined to be 5 μg·mL$^{-1}$ [19].

### 1.7 Zebrafish culture and embryo selection

Adult zebrafish with fluorescent tags for research were obtained from Southern Medical University (Guangzhou, China). Fish were fed with commercially fish food twice daily and kept at a 14 h light/10 h dark photoperiod. On the evening before spawning, two male and one female adult fish were placed in each of the 5 hatching boxes, and spawning was prompted when the light was turned on in the next morning. The fertilized eggs were washed twice with fish culture medium and examined under a stereo microscope (Olympus-SZ61, Japan). The embryos that had developed normally and reached the blastula stage were sorted and pooled for the subsequent experiments[20].

### 1.8 Exposure experiment by zebrafish

The toxicity tests of compound **1** at different concentrations were conducted as follows: included two groups, the control group (culture medium) and **1** exposure group (0, 31.25, 62.5, 125 and 250 μg·mL$^{-1}$). Then embryos were transferred into 24-well plates (Costar® 24-Well Cell Culture Cluster, Corning Incorporated, USA), one embryo per well and each plate included 20 embryos for exposure test and 4 embryos as internal fish water control. Then the plates were placed in an illumination incubator at (28±1) ℃ with a 14 h light/10 h dark photoperiod. **1** suspensions were renewed at 24 h intervals during the experimental period. The observation was performed in the well under a stereo microscope (Olympus, Japan) equipped with a digital camera at specified time points ($t$=24, 48 h). The endpoints used to assess developmental toxicity included whether embryo/larvae were malformed[21].

Live subject statement: The experimental protocol involving handling and treatment of zebrafish embryos and larvae was in accordance with the National Institute of Health′s Guide for the Care and Use of Laboratory Animals, China.

## 2 Results and discussion

### 2.1 Structure description

Single-crystal X-ray diffraction measurement shows that compound **1** crystallizes in the orthorhombic *Cmca* space group, and the asymmetric unit of **1** contains half a Zn(Ⅱ) ions, half a BDC anion, half a dmbpy ligand and two free water molecules. Zn1 is four-coordinated by two carboxylate oxygen atoms from two different BDC anions, two nitrogen atoms from two different dmbpy ligands, adopting a distorted tetrahedral coordination geometry (Fig.1a) with Zn-O, Zn-N bond distances and O-Zn-O, O-Zn-N, N-Zn-N bond angles ranging from 0.198 2(3) to 0.204 9(3) nm and from 100.55(17)° to 116.31(11)°, respectively. The values are in agreement with those found in other four-coordinated Zn(Ⅱ) complexes with oxygen and nitrogen donating ligands[22]. In the crystal structure of **1**, the BDC ligand links two metal ions with bridging-monodentate-$\mu_2$ mode, whereas dmbpy ligand acts as a *trans*-bidentate bridging ligand to link two Zn(Ⅱ) ions. In this manner, a 2D (4,4) network with 1D channel of 0.92 nm×0.83 nm and 0.82 nm×0.39 nm along the *b* axis (measured between opposite atoms), respectively, has been constructed from the 1D Zn(Ⅱ)-carboxylate chains and dmbpy pillars (Fig.1b and 1c). Finally, adjacent layers are further interconnected via C4–H4 ⋯Cg1 (Cg1=centroid of N1/C9-C13 ring) stacking interactions, C13–H13 ⋯ O1 and C13–H13 ⋯ O2 hydrogen bonds involving carboxylate O atoms to form a three-dimensional supramolecular network (Table 3). Topologically, the zinc center acts as 4-connected node, the BDC and dmbpy ligands act as linker, respectively. Compound **1** represents a $4^4$-*sql* net. The potential voids is 0.984 8 nm$^3$, which is about 22.4% of the unit cell volume[17].

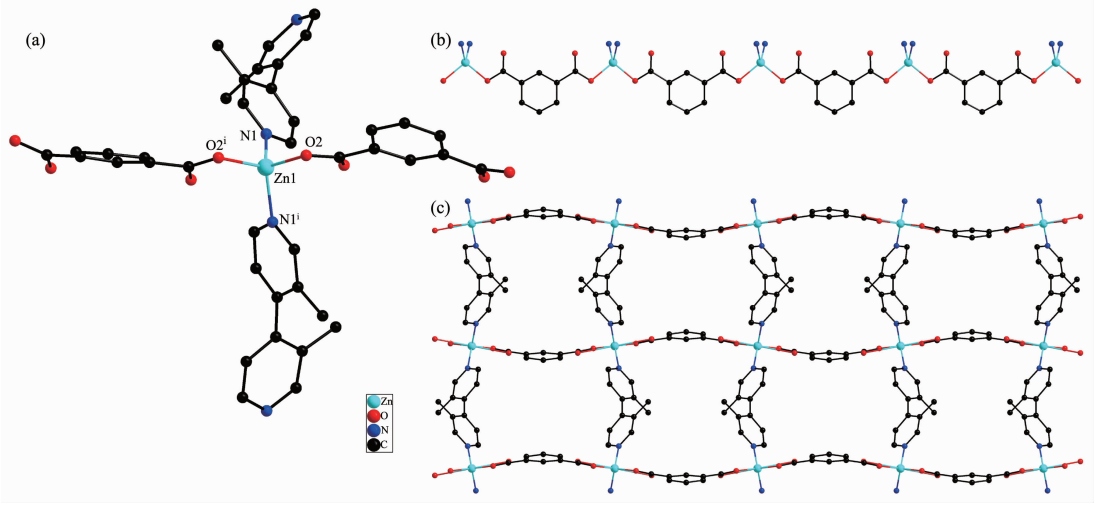


All H atoms are omitted for clarity; Symmetry code: ⁱ 0.5–*x*, *y*, 0.5–*z*

Fig.1 (a) Coordination environment for Zn(Ⅱ) ion in **1**; (b) View of an infinite Zn(Ⅱ)-carboxylate chain of **1**; (c) View of 2D framework of **1**

### 2.2 Powder X-ray diffraction analysis

Bulk samples were also measured by X-ray diffraction at room temperature to check the purity of **1**. As shown in Fig.2, all major peaks of the experimental PXRD patterns of compound **1** matched well that of simulated PXRD patterns, which clearly indicates the high purity of the compound.

Furthermore, the stabilities of **1** in aqueous solutions were investigated by PXRD (Fig.2).

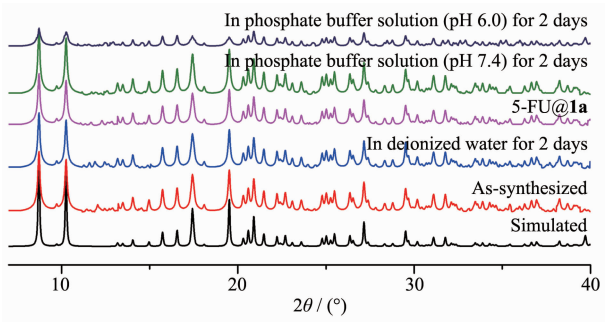


Fig.2 PXRD patterns for **1**

According to these results, compound **1** is stable in aqueous solutions and PBS (pH=7.4) but unstable in acidic environment (pH=6.0). The results is remarkable when compared with other MOFs constructed from aromatic carboxylate and transition metal ions[23].

### 2.3 IR and thermogravimetric analysis

FT-IR spectra were recorded as KBr pellets (Fig. S1). The IR spectrum of **1** showed adsorption band at 3 387 $cm^{-1}$ (for O-H stretching vibrations of the water molecules), 3 012 $cm^{-1}$ (for C-H stretching vibrations of benzene rings from BDC and dmbpy ligands), 2 958 $cm^{-1}$ (for C-H stretching vibrations of -$CH_3$ from dmbpy ligands). The strong and sharp bands at 1 610 and 1 357 $cm^{-1}$ are associated with the asymmetric (C-O-C) and symmetric (C-O-C) stretching vibrations. The IR spectra of 5-FU and 5-FU@**1a** showed prominent characteristic absorption bands of 5-FU at 3 015 $cm^{-1}$ (for N-H), 2 800~3 000 $cm^{-1}$ (for C-H), 1 745 $cm^{-1}$ (for C=O), 1 697 $cm^{-1}$ (for C-F). Compared with 5-FU parent, the broadening, weakening and shift of some features absorption peak intensity indicate that 5-FU have been successfully loaded into the new carrier **1a**.

To test the thermal stability of **1**, we performed the thermogravimetric analysis (Fig.3). The TG analysis curve for compound **1** showed a weight loss of about 15.1% in the temperature range of 50~120 ℃, which corresponds to the loss of four free water molecules (Calcd. 14.8%). The compound begins to decompose when the temperature is raised to 320 ℃. Finally, compound **1** was completely degraded into ZnO.

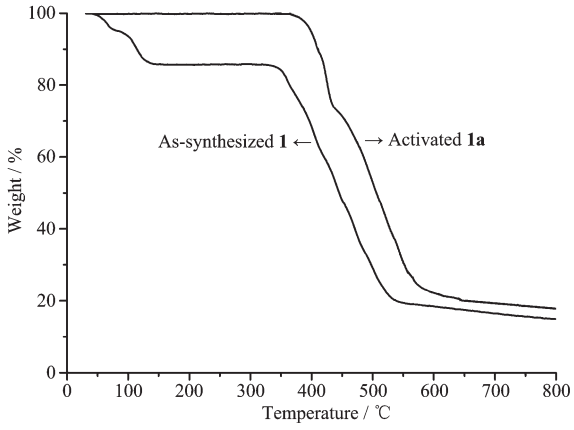


Fig.3 Thermogravimetric curves of **1** and **1a**

### 2.4 $N_2$ sorption isotherms

$N_2$ sorption measurements were used to examine the porosity of the MOF samples after being soaked in water for 2 days. **1** was activated (**1a**) at 130 ℃ for 12 h under vacuum. The $N_2$ sorption isotherms was performed at 77 K and showed a Ⅰ-type isotherm characteristic of a microporous material (Fig.4) with the BET surface area of 240 $m^2 \cdot g^{-1}$. No significant loss in the BET surface area was observed (from 240 to 220 $m^2 \cdot g^{-1}$) for **1** after being soaked in water for 2 days, indicating the maintenance of the porous structures of **1** in water.

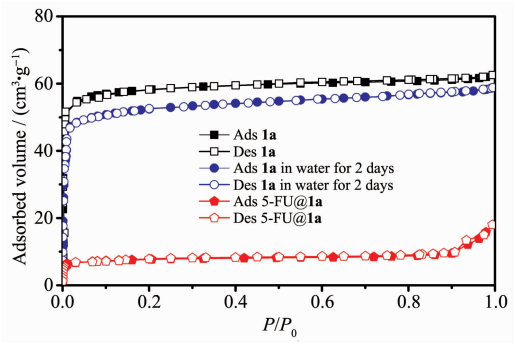


Fig.4 Nitrogen sorption isotherm at 77 K

### 2.5 Drug delivery studies

$N_2$ adsorption measurements (HK models) indicated that the pore size of **1** was 0.81 nm (Fig.S2). Compound **1**, with wide-open channels (0.92 nm × 0.83nm and 0.82 nm×0.39 nm) is suitable for loading of 5-FU with the molecular size of 0.53 nm×0.5 nm[24]. Incorporation of the 5-FU molecule during the adsorption process was confirmed by FT-IR and $N_2$ sorption (Fig.S1 and 4). The BET surface area of the 5-FU loaded MOF is 23 $m^2 \cdot g^{-1}$, which show *ca.* 90.4% reduction, as compared with the as-synthesized sample (240 $m^2 \cdot g^{-1}$). The result indicates that there is almost no residual porosity after the drug adsorption, thus the 5-FU molecules approximately filled up the pores and channels. UV-Vis was used to determine the effective storage capacity of **1a**. To achieve a maximal drug loading of 5-FU to the pore solid, mass ratio of 5-FU to porous solid and contact time were tested (Table 4). It was observed that the best result was achieved by dissolving 5 mg of 5-FU into 10 mL of methanol, then 10 mg of **1a** ($m_{5\text{-FU}}$:$m_{\mathbf{1a}}$=1:2) was added into the solution and vortexed at 3 000 r·$min^{-1}$ for 20 min. HPLC analysis indicates that the desolvated **1** shows a 5-FU absorption capacity with the encapsulation efficiency

**Table 4　Encapsulation efficiency of 5-FU affected by mass ratio of 5-FU to 1a and contact time**

| $m_{5\text{-FU}}$:$m_{\mathbf{1a}}$ | Contact time / min | Encapsulation efficiency / %(*w*/*w*) |
|---|---|---|
| 1:1 | 5, 10, 20, 30 | 6.3, 8.1, 7.5, 5.2 |
| 1:2 | 5, 10, 20, 30 | 7.2, 11.1, 14.2, 10.5 |
| 1:3 | 5, 10, 20, 30 | 9.4, 12.1, 10.9, 8.7 |
| 2:1 | 5, 10, 20, 30 | 7.2, 8.7, 6.2, 5.6 |
| 2:3 | 5, 10, 20, 30 | 4.8, 5.6, 7.8, 8.2 |
| 3:1 | 5, 10, 20, 30 | 7.4, 8.8, 9.5, 11.4 |
| 3:2 | 5, 10, 20, 30 | 5.2, 6.8, 5.6, 6.1 |

of 14.2%(*w*/*w*), which is lower than the 5-FU loading in the reported literatures with the similar pore size, but the result is very remarkable when compared with those 3D MOFs with the BET surface of some times larger than **1a**[24-27]. Moreover, the amount of 5-FU in the sample was determined by TGA and elemental analysis. The TGA curve was depicted in Fig.S3. A weight-loss of 2.1% was observed from 100 to 180 ℃, which is assigned to the loss of residual water molecules. Upon further heating, a weight-loss of 13.5% was observed from 180 to 250 ℃, due to the release of 5-FU molecules. The sharp weight-loss step that occurred above 330 ℃ corresponds to the decomposition of the framework. Elemental analysis technique was employed to obtain the organic species (C, H) of the dried 5-FU-loaded **1a**. The result indicated a 5-FU content of 14.7%(*w*/*w*) on the basis of the data (C 55.0%; H 5.8 %, N 8.6%).

The 5-FU drug release profiles from drug-loaded **1a** were studied *in vitro* by the dialysis method. Meanwhile, the 5-FU release from the free drug suspension was investigated as control group. As shown in Fig.5, in the control group, during the first 6 h, over 96% of the 5-FU drug was released from the drug suspension. Then in the following 4 h, the accumulative release value of 5-FU reached 100%. For 5-FU@**1a**, the delivery of 5-FU occurred within 20 h with no "burst effect". The drug release rates were 94.5% (pH=7.4) and 99% (pH=6.0) of drug release after 72 and 28 h, respectively. Two distinct stages of the drug release can be observed: 62% (0~28 h, pH=7.4), 76% (0~13 h, pH=6.0) in first stage and 32.5% (28~70 h, pH=7.4), 24% (15~30 h, pH=6.0) in last stage. The release time of 5-FU (pH=7.4) in **1a** is longer than that of reported MOFs with similar pore size[24-27]. The relatively slow release might attributed to the hydrogen-bonding interactions (N–H···O, C–H···O, C–H···F) and $\pi\cdots\pi$ stacking interactions involving the 5-FU molecules and the pore chemical environment[14,25,27]. The slightly fast-release in low pH condition (pH=6.0) may result from the degradation of the structure.

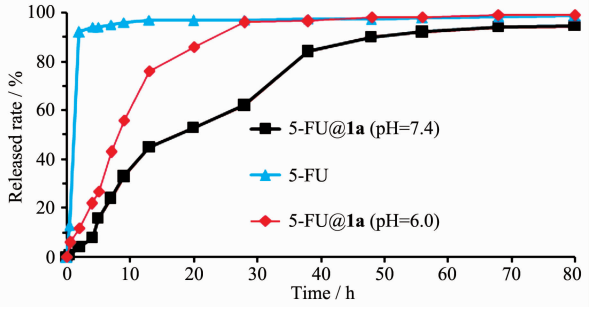


Fig.5　Release of 5-FU from the drug-loaded **1a** and control experiment

## 2.6　MTT tests and zebrafish tests

MTT toxicity assays were taken from two different normal cells lines (HEK-293 and NIH-3T3) and two different cancer lines (A549 and HEPG2) with increasing concentrations of **1a**. The results revealed that the compound **1** was nontoxic (Cell viability > 80%) when the concentrations were below 500 μg·mL$^{-1}$ for 24 and 48 h (Fig.S4 and S5).

The toxicity tests of **1** at different concentrations were also investigated. As shown in Fig.6, the zebrafish in the control group showed a normal appearance after 24 and 48 h, respectively, including clear blood vessels with fluorescent tags, straight spine and no pericardium edema, *etc*. While exposure to **1** (Concentration: below 125 μg·mL$^{-1}$ for 24 h and below 62.5 μg·mL$^{-1}$ for 48 h) caused no remarkable morphological abnormalities compared with the control group. These results suggest that **1** is not toxicity to zebrafish under certain concentration and residence time.

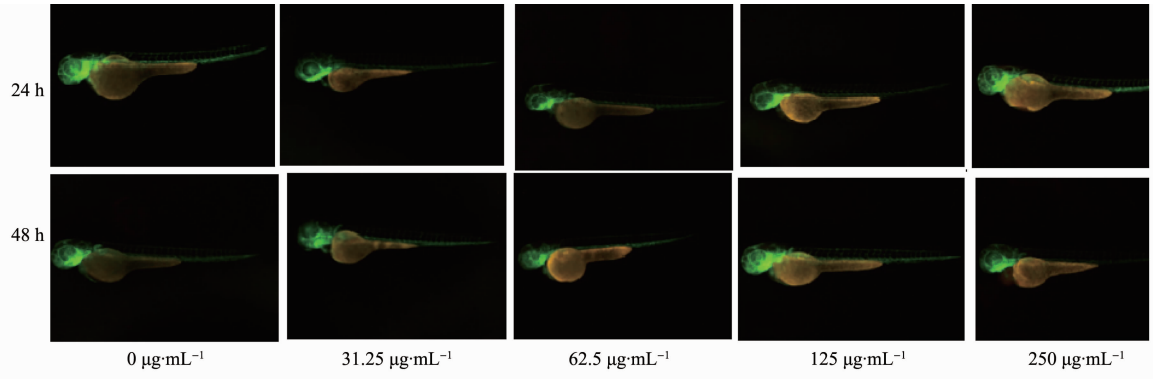


Fig.6 Zebrafish toxicity tests for **1** with different concentrations

## 3 Conclusions

In summary, a water-stable 2D MOF with the channels of 0.92 nm×0.83 nm and 0.82 nm×0.39 nm was constructed from isophthalate and 3,3′-dimethyl-4,4′-bipyridine ligands under hydrothermal condition. De-solvated **1** shows a 14.2%(*w*/*w*) 5-FU payload and performs a progressive release of the drug without any "burst effect" with a full release of 5-FU achieved in PBS after about 70 h (pH=7.4) and 28 h (pH=6.0), respectively. The MTT arrays and zebrafish toxicity tests show that **1** is nontoxic under certain concentration and residence time.

Supporting information is available at http://www.wjhxxb.cn

## References:

[1] Banerjee D, Elsaidi S K, Thallapally P K. *J. Mater. Chem. A*, **2017**,**5**:16611-16615

[2] Lee S J, Kim S, Kim E J, et al. *Chem. Eng. J.*, **2018**,**335**:345-351

[3] Medishetty R, Zareba J K, Mayer D, et al. *Chem. Soc. Rev.*, **2017**,**46**:4976-5004

[4] (a)Chen L F, Xu Q. *Science*, **2017**,**358**:304-305
(b)LIU Yuan-Yuan(刘媛媛)), LI Xin-Shu(李欣书), ZHANG Hui-Min(张慧敏), et al. *Chinese J. Inorg. Chem.*(无机化学学报), **2018**,**35**(12):2280-2290

[5] Espallargas G M, Coronado E. *Chem. Soc. Rev.*, **2018**,**47**:533-557

[6] (a)Zheng K, Liu Z Q, Chen F, et al. *Sens. Actuators B*: *Chem.*, **2018**,**257**:705-713
(b)LU Yan-Lei(卢延磊), ZHU Ning(朱宁), ZHAO Yu-Meng(赵宇萌), et al. *Chinese J. Inorg. Chem.*(无机化学学报), **2019**,**35**(4):720-728

[7] Ma D Y, Xie J, Zhu Z, et al. *Inorg. Chem. Commun.*, **2017**,**86**:128-132

[8] Zhang X J, Wang W J, Hu Z J, et al. *Coord. Chem. Rev.*, **2015**,**284**:206-235

[9] Yu Y J, Yu C, Niu Y Z, et al. *Biosens. Bioelectron.*, **2018**,**101**:297-303

[10]Assen A H, Yassine O, Shekhah O. *ACS Sens.*, **2017**,**2**:1294-1301

[11]Ma D Y, Li Y W, Li Z. *Chem. Commun.*, **2011**,**47**:7377-7379

[12]Mitra S, Sasmal H S, Kundu T, et al. *J. Am. Chem. Soc.*, **2017**,**139**:4513-4520

[13]Keskin S, Kizilel S. *Ind. Eng. Chem. Res.*, **2011**,**4**:1799-1812

[14]Horcajada P, Serre C, Vallet-Regi M, et al. *Angew. Chem. Int. Ed.*, **2006**,**118**:6120-6124

[15]*APEX* Ⅱ *Software*, *Vers*. 6.3.1, Bruker AXS Inc, Madison, Wisconsin, USA, **2004**.

[16]Sheldrick G M. *Acta Crystallogr. Sect. A*: *Found. Crystallogr.*, **2008**,**A64**:112-122

[17]Spek A L. *PLATON, A Multipurpose Crystallographic Tool*, Utrecht University, The Netherlands, **2005**.

[18]Wang J, Ma D Y, Liao W L, et al. *CrystEngComm*, **2017**,**19**:5244-5250

[19]Chalati T, Horcajada P, Couvreur P, et al. *Nanomedicine*, **2011**,**6**:1683-1695

[20]Zhao X S, Wang S T, Wu Y, et al. *Aquat. Toxicol.*, **2013**,**136-137**:49-59

[21]Chen T H, Lin C C, Meng P J. *J. Hazard. Mater.*, **2014**,**277**:134-140

[22]Ma D Y, Lu K, Qin L, et al. *Inorg. Chim. Acta*, **2013**,**396**:84-91

[23]Sun C Y, Qin C, Wang C G, et al. *Adv. Mater.*, **2011**,**23**:5629-5632

[24]Li Q L, Wang J P, Liu W C, et al. *Inorg. Chem. Commun.*, **2015**,**55**:8-10

[25]Bag P P, Wang D, Chen Z, et al. *Chem. Commun.*, **2016**,**52**:3669-3672

[26]Liu J Q, Li X F, Gu C Y, et al. *Dalton Trans.*, **2015**,**44**:19370-19382

[27]Liu J Q, Wu J, Jia Z B, et al. *Dalton Trans.*, **2014**,**43**:17265-17273